Available online at www.sciencedirect.com
ScienceDirect
Journal of Organometallic Chemistry 692 (2007) 5777–5787
Journal of Organometallic Chemistry
www.elsevier.com/locate/jorganchem

(1,2,3,4,7-Pentamethylindenyl)rhodium complexes with arene ligands

Dmitry A. Loginov [a], Mikhail M. Vinogradov [a], Zoya A. Starikova [a], Elena A. Petrovskaya [a], Piero Zanello [b], Franco Laschi [b], Fulvio Rossi [b], Arnaldo Cinquantini [b], Alexander R. Kudinov [a,*]

[a] A. N. Nesmeyanov Institute of Organoelement Compounds, Russian Academy of Sciences, 28 ul. Vavilova, 119991 Moscow GSP-1, Russian Federation
[b] Dipartimento di Chimica, Universita di Siena, Via Aldo Moro, 53100 Siena, Italy

Received 5 June 2007; received in revised form 27 September 2007; accepted 4 October 2007
Available online 9 October 2007

Abstract

The reaction of $(\eta^5\text{-}C_9H_2Me_5)Rh(1,5\text{-}C_8H_{12})$ (**1**) with I_2 gives the iodide complex $[(\eta^5\text{-}C_9H_2Me_5)RhI_2]_2$ (**2**). The solvate complex $[(\eta^5\text{-}C_9H_2Me_5)Rh(MeNO_2)_3]^{2+}$ (generated *in situ* by treatment of **2** with Ag^+ in nitromethane) reacts with benzene and its derivatives giving the dicationic arene complexes $[(\eta^5\text{-}C_9H_2Me_5)Rh(arene)]^{2+}$ [arene = C_6H_6 (**3a**), C_6Me_6 (**3b**), C_6H_5OMe (**3c**)]. Similar reaction with the borole sandwich compound $CpRh(\eta^5\text{-}C_4H_4BPh)$ results in the arene-type complex $[CpRh(\mu\text{-}\eta^5\text{:}\eta^6\text{-}C_4H_4BPh)Rh(\eta^5\text{-}C_9H_2Me_5)]^{2+}$ (**4**). Treatment of **2** with CpTl in acetonitrile affords cation $[(\eta^5\text{-}C_9H_2Me_5)RhCp]^+$ (**5**). The structure of [**3c**]$(BF_4)_2$ was determined by X-ray diffraction. The electrochemical behaviour of complexes prepared was studied. The rhodium–benzene bonding in series of the related complexes $[(ring)Rh(C_6H_6)]^{2+}$ (ring = Cp, Cp*, C_9H_7, $C_9H_2Me_5$) was analyzed using energy and charge decomposition schemes.

Keywords: Electrochemistry; Indenyl complexes; Rhodium; Sandwich complexes

1. Introduction

Dicationic rhodium and iridium arene complexes $[Cp^*M(arene)]^{2+}$ are known for more than 35 years [1]. They have attracted much attention because of high reactivity of the arene ligands toward nucleophilic reagents. In particular, they were used as catalysts for nucleophilic substitution of the fluorine atom in the benzene ring [2] and as reagents in a closed cycle of benzene reduction to cyclohexene [3].

Recently, we have synthesized analogous arene complexes with unsubstituted cyclopentadienyl ring $[CpM(arene)]^{2+}$ (M = Rh, Ir) by reaction of solvate complexes $[CpM(MeNO_2)_3]^{2+}$ (generated *in situ* by treatment of $[CpMI_2]_2$ with Ag^+ in nitromethane) with arenes [4]. The iridium cation $[CpIr(\eta\text{-}C_6H_6)]^{2+}$ exhibits a catalytic activity in reactions of alkane oxidation by *m*-chloroperoxybenzoic acid [5]. In a similar manner, we have prepared metallacarborane derivatives $[(\eta\text{-}9\text{-}SMe_2\text{-}7,8\text{-}C_2B_9H_{10})M(arene)]^{2+}$ (M = Rh, Ir) from bromides $[(\eta\text{-}9\text{-}SMe_2\text{-}7,8\text{-}C_2B_9H_{10})MBr_2]_2$ [6].

The related arene complexes of the (indenyl)rhodium fragment are presently unknown, in spite of rather well study of chemistry of this fragment [7–10]. Herein, we report the synthesis of (1,2,3,4,7-pentamethylindenyl)rhodium arene complexes $[(\eta^5\text{-}C_9H_2Me_5)Rh(arene)]^{2+}$ as well as the results of their structural and electrochemical study.

2. Results and discussion

2.1. Synthesis

Similar to the previously reported synthesis of iodide $[CpRhI_2]_2$ [4], the pentamethylindenyl analogue $[(\eta^5\text{-}C_9H_2Me_5)RhI_2]_2$ (**2**) was prepared by treatment of the cyclooctadiene complex $(\eta^5\text{-}C_9H_2Me_5)Rh(1,5\text{-}C_8H_{12})$ (**1**) with I_2 (Scheme 1). The starting compound **1** was synthesized by

* Corresponding author. Tel.: +7 495 135 9367; fax: +7 495 135 5085.
E-mail address: arkudinov@ineos.ac.ru (A.R. Kudinov).

0022-328X/$ - see front matter © 2007 Elsevier B.V. All rights reserved.
doi:10.1016/j.jorganchem.2007.10.006

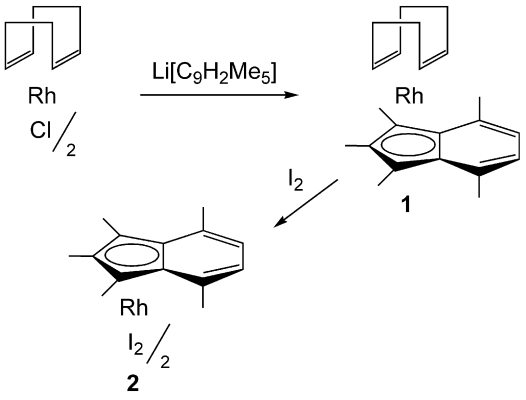

Scheme 1.

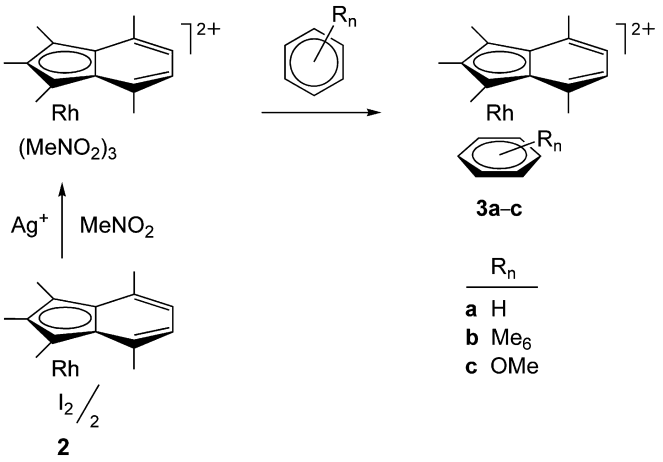

Scheme 2.

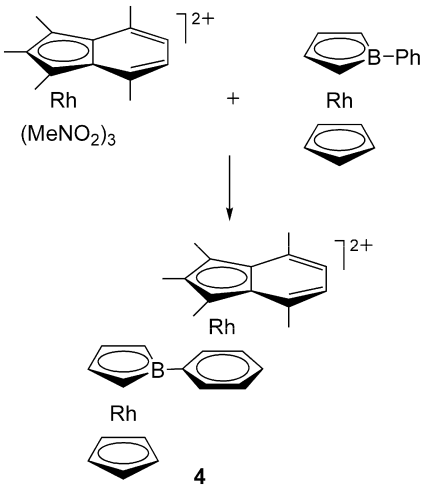

Scheme 3.

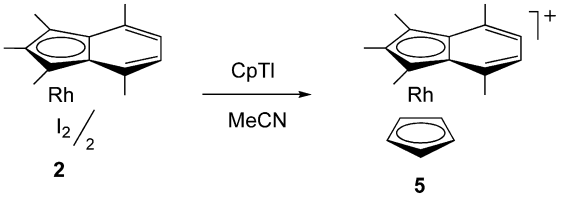

Scheme 4.

reaction of $[(1,5\text{-}C_8H_{12})RhCl]_2$ with 1,2,3,4,7-pentamethylindenyl lithium.

We found that the reaction of the solvate complex $[(\eta^5\text{-}C_9H_2Me_5)Rh(MeNO_2)_3]^{2+}$ (generated *in situ* by treatment of **2** with Ag^+ in nitromethane) with benzene and its derivatives affords the dicationic arene complexes $[(\eta^5\text{-}C_9H_2Me_5)Rh(arene)]^{2+}$ (**3a**–**c**) (Scheme 2).[1] Unfortunately, our attempts to prepare similar complexes with unsubstituted indenyl ligand $[(\eta^5\text{-}C_9H_7)Rh(arene)]^{2+}$ in the same conditions were unsuccessful.

The related arene complexes $[(\eta\text{-}C_5R_5)Rh(arene)]^{2+}$ (R = H, Me) and $[(\eta\text{-}9\text{-}SMe_2\text{-}7,8\text{-}C_2B_9H_{10})Rh(arene)]^{2+}$ are known to readily undergo arene replacement by solvent molecules, Me_2CO and MeCN [1,4,6,11]. For example, benzene in $[Cp^*Rh(\eta\text{-}C_6H_6)]^{2+}$ is completely displaced by acetone within 30 min at room temperature [11]. The parent cation $[CpRh(\eta\text{-}C_6H_6)]^{2+}$ completely transforms into $[CpRh(MeCN)_3]^{2+}$ in acetonitrile within 15 min; similar transformation in acetone takes 2 h [4]. In contrast, the indenyl analogue **3a** is stable in MeCN for at least one week.

Recently, we have shown that the reactions of cationic fragments $[(ring)M]^{n+}$ $(n = 1, 2)$ with the B-phenylborole complex $CpRh(\eta^5\text{-}C_4H_4BPh)$ give either triple-decker or arene-type complexes [12,13]. The reaction of $[(\eta^5\text{-}C_9H_2Me_5)Rh(MeNO_2)_3]^{2+}$ with $CpRh(\eta^5\text{-}C_4H_4BPh)$ results in the arene-type complex $[CpRh(\mu\text{-}\eta^5{:}\eta^6\text{-}C_4H_4BPh)Rh(\eta^5\text{-}C_9H_2Me_5)]^{2+}$ (**4**) (Scheme 3), similar to reaction with $[Cp^*Rh(MeNO_2)_3]^{2+}$.

Iodide **2** can be also used directly (without preliminary generation of solvates) as a synthon of the $(\eta^5\text{-}C_9H_2Me_5)Rh$ species. For example, the reaction of **2** with CpTl in acetonitrile results in the sandwich cation $[(\eta^5\text{-}C_9H_2Me_5)RhCp]^+$ (**5**) (Scheme 4).

2.2. Structure of $[3c](BF_4)_2$

The molecular structure of complex $[\mathbf{3c}](BF_4)_2$ consists of separated cation **3c** and two BF_4^- anions. Cation has the expected sandwich structure (Fig. 1). Selected bond lengths and angles are given in Table 1.

The structure of cation **3c** is the first example of (indenyl)(arene)rhodium complex. The rhodium atom is not quite symmetrically coordinated with the five-membered ring, the distances from the Ru atom to the bridgehead C4 and C9 atoms (2.212 Å) being noticeably longer than other Rh–C distances (av. 2.168 Å). The elongation value (0.044 Å) is in the range for true η^5-indenyl complexes

[1] All the cationic complexes described here were isolated as salts with the BF_4^- or PF_6^- anions.

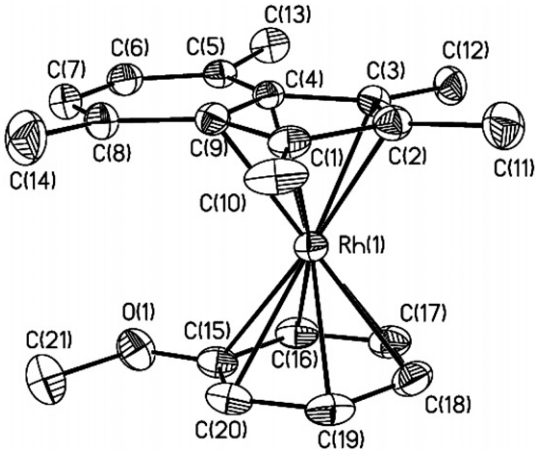

Fig. 1. Structure of cation **3c**.

Table 1
Selected bond lengths (Å) and angles (°) for cation **3c**

Rh(1)–C(1)	2.157(3)	C(1)–C(2)	1.446(4)
Rh(1)–C(2)	2.189(3)	C(2)–C(3)	1.444(4)
Rh(1)–C(3)	2.157(3)	C(3)–C(4)	1.450(4)
Rh(1)–C(4)	2.212(3)	C(4)–C(9)	1.456(3)
Rh(1)–C(9)	2.212(3)	C(1)–C(9)	1.452(4)
Rh(1)–C(15)	2.353(3)	C(4)–C(5)	1.438(4)
Rh(1)–C(16)	2.287(3)	C(5)–C(6)	1.371(4)
Rh(1)–C(17)	2.251(3)	C(6)–C(7)	1.423(4)
Rh(1)–C(18)	2.220(3)	C(7)–C(8)	1.367(4)
Rh(1)–C(19)	2.240(3)	C(8)–C(9)	1.440(4)
Rh(1)–C(20)	2.293(3)		
C(1)–C(2)–C(3)	108.6(2)	C(5)–C(6)–C(7)	122.7(3)
C(2)–C(3)–C(4)	107.6(2)	C(6)–C(7)–C(8)	123.4(3)
C(3)–C(4)–C(9)	108.0(2)	C(7)–C(8)–C(9)	116.6(3)
C(1)–C(9)–C(4)	107.8(2)	C(4)–C(9)–C(8)	119.9(2)
C(9)–C(1)–C(2)	107.6(2)	C(9)–C(4)–C(5)	121.2(2)
C(4)–C(5)–C(6)	116.2(2)		

[14–16]. The five-membered ring is folded along the line C1–C3 (5.9°).

The Rh $\cdots$ C_6H_5R plane distance in **3c** (1.776 Å) is longer than those for $[Cp^*Rh(C_6H_5R)]^{2+}$ (R = Me [17], NH_2 [18], $(BC_4H_4)RhCp$ [12]) (1.766, 1.758 and 1.760 Å, respectively) in accordance with poorer benzene bonding with the $[(\eta^5\text{-}C_9H_2Me_5)Rh]^{2+}$ than with $[Cp*Rh]^{2+}$ (vide infra).

2.3. Electrochemistry

Fig. 2 shows the cyclic voltammetric response exhibited by the Rh(I) complex **1** in dichloromethane solution. In agreement with the redox behaviour of the related complex $(\eta^5\text{-}C_5Ph_5)Rh(1,5\text{-}C_8H_{12})$ [19], it undergoes two subsequent one-electron oxidations exhibiting features of chemical reversibility in the cyclic voltammetric time scale (or, the pertinent i_{pc}/i_{pa} ratios are constantly equal to 1 with the scan rates progressively increasing from 0.02 to 10.2 V s^{-1}) [20], but in the longer times of macroelectrolysis only the monocation proved to be quite stable, as testified

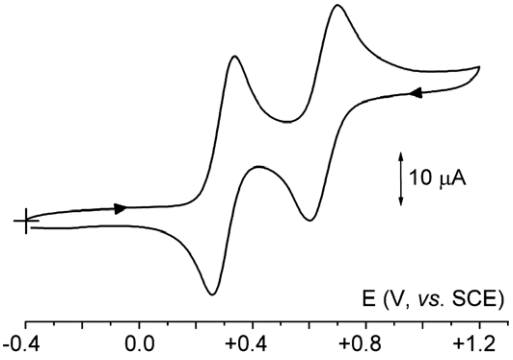

Fig. 2. Cyclic voltammetric profile recorded at a gold electrode in CH_2Cl_2 solution of **1** (1.4×10^{-3} mol dm^{-3}). $[NBu_4][PF_6]$ (0.2 mol dm^{-3}) supporting electrolyte. Scan rate 0.05 V s^{-1}. $T = 290$ K.

by cyclic voltammetry which afforded profiles quite complementary to the original ones. It is noted that the unsubstituted complex $(\eta^5\text{-}C_9H_7)Rh(1,5\text{-}C_8H_{12})$ only exhibits a partially chemically reversible one-electron oxidation [21]. Unfortunately, in contrast to the detailed investigations carried out on the reduction processes of $(\eta^5\text{-}C_5Ph_5)Rh(1,5\text{-}C_8H_{12})$ and $(\eta^5\text{-}C_9H_7)Rh(1,5\text{-}C_8H_{12})$ [19,22], we could not study the cathodic activity of **1** because it was substantially masked by the solvent discharge.

Upon exhaustive one-electron oxidation, the original pale yellow solution of **1** turns gold yellow and tends to adsorb at $\lambda \approx 400$ nm (Fig. 3).

As deducible from Table 2, which compiles the formal electrode potentials of the redox processes exhibited by the species under study, the indenyl methylation markedly favours the access to the Rh(II) and Rh(III) cations, as well as stabilizes the Rh(II) monocation.

In propylene carbonate solution, the first one-electron oxidation of **1** is accompanied by a slow chemical complication (generating an irreversible oxidation at about

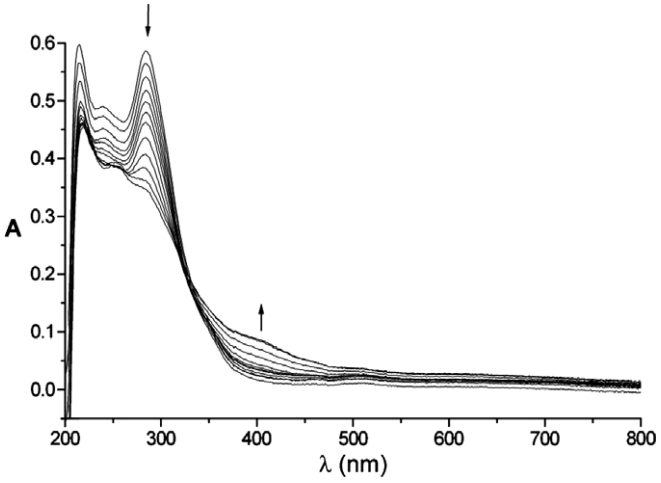

Fig. 3. UV–Vis spectral trend recorded in a OTTLE cell upon stepwise oxidation of **1** in CH_2Cl_2 solution. $[NBu_4][PF_6]$ (0.2 mol dm^{-3}) supporting electrolyte. $T = 290$ K.

Table 2
Formal electrode potentials (V, vs. SCE) and peak-to-peak separations (mV) of the Rh(III)/Rh(II)/Rh(I) sequence in the (pentamethylindenyl)rhodium complexes under study, and related derivatives

Complex	$E^{\circ'}_{Rh(III)/Rh(II)}$	ΔE_p[a]	$E^{\circ'}_{Rh(II)/Rh(I)}$	ΔE_p[a]	Solvent	Temperature[b]
1	+0.65	126	+0.30	96	CH_2Cl_2	290
	+0.66	186	+0.27	138	CH_2Cl_2	253
	>+1.2[c]		+0.31[d]	64	PC[e]	290
5	−1.25	73	−1.80	92	PC[e]	290
	−1.27	93	−1.79	160	PC[e]	253
	−1.28	73	[f]		CH_2Cl_2	290
	−1.24	104	[f]		CH_2Cl_2	253
3a	−0.14[d,g]	128[g]	−0.76[d,g]	208[g]	PC[e]	253
	−0.13[d,g]	190[g]	−0.76[d,g]	210[g]	PC[e]	290
3b	−0.34	79	−0.92	66	PC[e]	253
	−0.31	59	−0.91	59	PC[e]	290
	−0.19	62	−0.95	71	CH_2Cl_2	253
	−0.16	71	−0.91[d]		CH_2Cl_2	290
3c	−0.20[d,g]	174[g]	−0.74[d,g]	236[g]	PC[e]	253
	−0.16[d,g]	168[g]	−0.73[d,g]	166[g]	PC[e]	290
$(\eta^5\text{-}C_9H_7)Rh(1,5\text{-}C_8H_{12})$			+0.56[d,h]	66	CH_2Cl_2	293
$(\eta^5\text{-}C_5Ph_5)Rh(1,5\text{-}C_8H_{12})$[i]	+1.18		+0.55		CH_2Cl_2	278
$[(\eta^5\text{-}C_9H_7)Rh(C_5Me_5)]^{+l}$	−1.18		−1.88		THF	303
$[(\eta^5\text{-}C_5Me_5)Rh(C_6H_6)]^{2+m}$	−0.42[d]				Me_2CO	298
$[(\eta^5\text{-}C_5Me_5)Rh(C_6Me_6)]^{2+m}$	−0.57[d]		−0.77[d]		Me_2CO	298

[a] Measured at 0.2 V s^{-1}.
[b] In K.
[c] Partially overlapped by the solvent discharge.
[d] Partial chemical reversibility.
[e] PC = propylene carbonate.
[f] Masked by the solvent discharge.
[g] Measured at 20.4 V s^{-1}.
[h] From Ref. [21].
[i] From Ref. [19].
[l] From Ref. [23].
[m] From Ref. [24].

+0.5 V, which progressively disappears with the increase of the scan rate).

Fig. 4 shows the cyclic voltammetric fingerprint of the Rh(III) monocation **5** in propylene carbonate solution. As expected on the basis of the electrochemical behaviour of either $[(C_5Me_5)Rh(C_5H_5)]^+$ or the unsubstituted indenyl analogue $[(\eta^5\text{-}C_9H_7)Rh(C_5Me_5)]^+$ [23], it undergoes the sequence Rh(III)/Rh(II)/Rh(I) through two separate steps

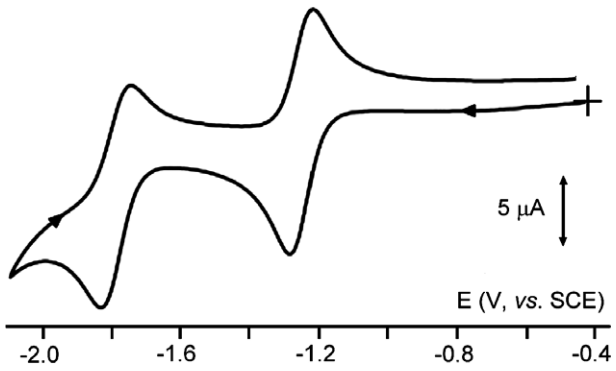

Fig. 4. Cyclic voltammetric profile recorded at a gold electrode in propylene carbonate solution of **5** (1.2×10^{-3} mol dm^{-3}). $[NBu_4][PF_6]$ (0.2 mol dm^{-3}) supporting electrolyte. Scan rate 0.05 V s^{-1}. $T = 290$ K.

featuring chemical reversibility in the cyclic voltammetric time scale. The first reduction proved to be chemically reversible also in the electrolysis time scale, even if we did not succeed to complete the one-electron addition because of the slow continuous reoxidation at the macroelectrolysis electrode, probably triggered by traces of air. No appreciable change of the original yellow color as well as of the spectral pattern (but for a decrease of the starting peak at 290 nm) were detected upon progressive reduction. In dichloromethane solution, the most cathodic process is substantially overlapped to the solvent discharge.

Let us finally pass to the arene-Rh(III) dications **3a–c**. As happens for the related complexes $[(arene)Rh(C_5Me_5)]^{2+}$ [24], the nature of the substituents present at the benzene ring significantly affects the kinetic stability of the pertinent Rh(II) and Rh(I) oxidation states. In fact, as illustrated in Fig. 5, the sequence Rh(III)/Rh(II)/Rh(I) is coupled to relatively fast chemical complications even at low temperature (253 K) in the case of the benzene complex **3a**, whereas in the case of the hexamethylbenzene analogue **3b** it proceeds though two simple electron transfers even at ambient temperature. The anisole complex **3c** substantially behaves as **3a**.

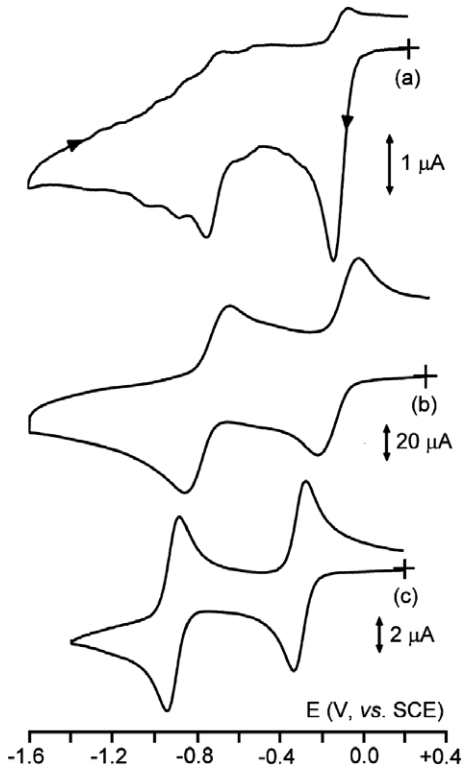

Fig. 5. Cyclic voltammetric profiles recorded at a platinum electrode in propylene carbonate solution of: (a,b) **3a** (2.1×10^{-3} mol dm^{-3}); (c) **3b** (1.7×10^{-3} mol dm^{-3}). $[NBu_4][PF_6]$ (0.2 mol dm^{-3}) supporting electrolyte. Scan rates: (a,c) 0.1 V s^{-1}; (b) 20.4 V s^{-1}. Temperatures: (a,b) 253 K; (c) 290 K.

Exhaustive one-electron reduction of the orange solution of $[(\eta^5\text{-}C_9H_2Me_5)Rh^{III}(C_6Me_6)]^{2+}$ (**3b**) afforded the brick-red monocation $[(\eta^5\text{-}C_9H_2Me_5)Rh^{II}(C_6Me_6)]^{+}$. In this connection, Fig. 6 shows the pertinent spectral trend recorded upon stepwise reduction.

In conclusion, the redox ability of complex **3b** is substantially similar to that of $[(\eta^5\text{-}C_5Me_5)Rh(C_6Me_6)]^{2+}$, even if the indenyl-Rh(II) monocation $[(\eta^5\text{-}C_9H_2Me_5)Rh(C_6Me_6)]^{+}$ looks like to be indefinitely stable, whereas $[(\eta^5\text{-}C_5Me_5)Rh(C_6Me_6)]^{+}$ has a lifetime of about 30 min [24].

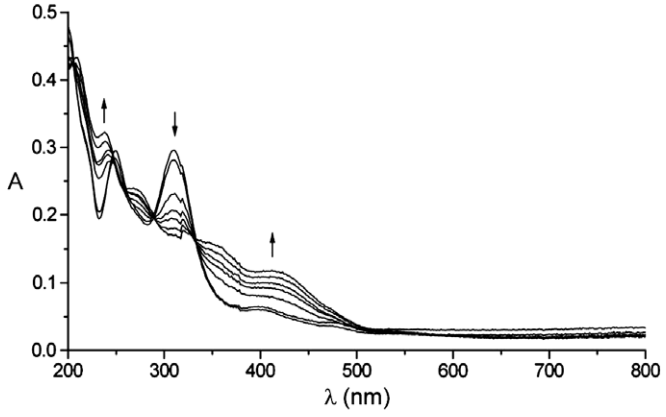

Fig. 6. UV–Vis spectral trend recorded in a OTTLE cell upon stepwise reduction of **3b** in PC solution. $[NBu_4][PF_6]$ (0.2 mol dm^{-3}) supporting electrolyte. $T = 290$ K.

2.4. EPR studies

As mentioned, the electrogenerated Rh(II) complexes $[(\eta^5\text{-}C_9H_2Me_5)Rh(1,5\text{-}C_8H_{12})]^{+}$, $[(\eta^5\text{-}C_9H_2Me_5)Rh(C_5H_5)]^{0}$, $[(\eta^5\text{-}C_9H_2Me_5)Rh(C_6Me_6)]^{+}$ proved to be quite stable, so that their EPR spectral properties have been investigated. As a typical example, Fig. 7 shows the X-band EPR spectrum of $[(\eta^5\text{-}C_9H_2Me_5)Rh(C_6Me_6)]^{+}$ recorded at liquid nitrogen temperature in PC solution.

The nice resolution of the three spectral regions testifies to the typical rhombic pattern. The anisotropic lineshape analysis can be suitably carried out in terms of Zeeman (g_i parameters), Hyperfine (hpf, a_i parameters) and Superhyperfine (shpf, a_i parameters) contributions to the general $S = 1/2$ electron spin Hamiltonian. The effective spin–orbit coupling of the Rh(II) center in low-spin state ($3d^7$, $S = 1/2$; doublet ground state; single electron calculated value of the $\lambda_{S.O.}$ of Rh(II) cation = 1220 cm^{-1}) [25,26] imparts a marked metallic character to the lineshape, as proved by the g_i values significantly different from those of the free electron ($g_{electron} = 2.0023$). In addition, the relatively large $\delta g_{\ell-h}$ parameter ($\delta g_{\ell-h} = g_\ell - g_h$) well supports a significant distortion of the actual Rh(II) coordinating framework.

Multiple derivative analysis (first–fourth derivative modes) joined with simulation procedures [27] allows us to gain the best fitted paramagnetic features of $[(\eta^5\text{-}C_9H_2Me_5)Rh(C_6Me_6)]^{+}$, particularly in the presence of the limited hyperfine (hpf) and/or superhyperfine (shpf) resolution of the anisotropic lineshapes. In particular, the g_ℓ absorptions of the second and third derivative modes are resolved in two significantly separated peaks (relative intensities = 1:1), while the third derivative mode of the g_m signal clearly puts in evidence the related a_m splitting.

The significant anisotropic splitting of the doublets is likely attributable to the direct hpf interaction of the unpaired spin density with the metal nucleus [100% of the magnetically active ^{103}Rh ($I = 1/2$)]. Accordingly, in the limit of the experimental anisotropic linewidths (ΔH_i), the multiple derivative analysis (fourth derivative) does not reveal further couplings (superhyperfine interaction, shpf) with the magnetically active nuclei of the ligand atoms (^{13}C, ^{1}H). An upper limit for such interactions (if any) can be evaluated as $\Delta H_i(^{13}C, ^{1}H) \geqslant a_i(^{13}C, ^{1}H)$. In reality, the lack of interaction of the unpaired electron of Rh(II) centres with magnetic donor atoms of coordination compounds is not unusual [19,28,29]. As a matter of the fact, the computed g_i values well account for the basic contribution of the Rh(II) 4d orbitals to the overall SOMO, being those of the donor atoms less effective in the limit of the experimental anisotropic linewidths.

At the glassy-fluid transition, the anisotropic signal drops out and a low intensity and noisy signal is detected,

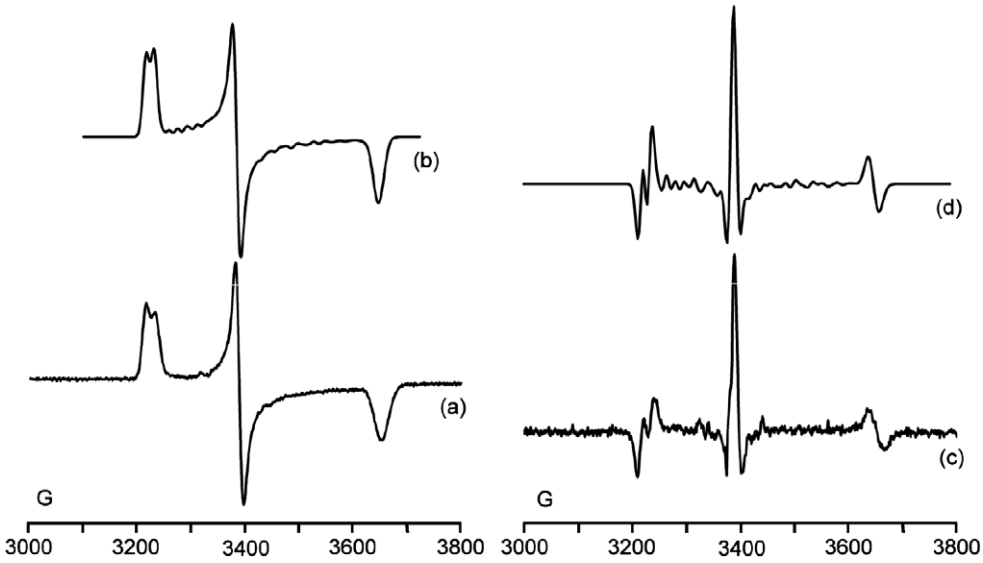

Fig. 7. X-band EPR spectra of $[(\eta^5\text{-}C_9H_2Me_5)Rh(C_6Me_6)]^+$ in PC solution, at 103 K. Experimental (a) and simulated (b) first derivative mode. Experimental (c) and simulated (d) second derivative mode. Operational $v = 9.457$ GHz.

the g_{iso} value of which well fits the related $\langle g \rangle$ one. Because of the low spectral resolution, the isotropic lineshape evidentiates a relatively broad doublet which confirms the basic hpf magnetic interaction of the unpaired spin density with the Rh(II) nucleus under fast motion condition. The pertinent g_{iso} and a_{iso} values are collected in Table 3, together with those of the other Rh(II) complexes here presented.

Quite similar paramagnetic features have been displayed by the low-spin Rh(II) $[(\eta^5\text{-}C_9H_2Me_5)Rh(C_5H_5)]^0$ in PC solution in spite of some noises both at liquid nitrogen and room temperatures. In fact, under glassy conditions, only the a_l and a_m splittings are resolved (second and third derivative modes), while the related g_h hpf interaction remains undetected. At the glassy-fluid transition, the anisotropic signal drops out and the solution becomes EPR mute. Accounting for the temperature dependent experimental linewidths, an upper limit for the different magnetic interactions can be proposed as $\Delta H_i(^{103}Rh, ^{13}C, ^1H) \geqslant a_i(^{103}Rh, ^{13}C, ^1H)$. It is noted that the related complex $[(\eta^5\text{-}C_9H_7)Rh(C_5Me_5)]^0$ in THF solution gives rise to an EPR spectrum with axial symmetry possessing a substantial metallic character too [23].

The fact that, in spite of the different overall charge, $[(\eta^5\text{-}C_9H_2Me_5)Rh^{II}(C_6Me_6)]^+$ and $[(\eta^5\text{-}C_9H_2Me_5)Rh^{II}(C_5H_5)]^0$ display similar EPR features suggests that the SOMO level of the two molecules is mainly contributed by the indenyl ligand.

Different temperature-dependent EPR features are displayed by the low-spin Rh(II) $[(\eta^5\text{-}C_9H_2Me_5)Rh(1,5\text{-}C_8H_{12})]^+$, in CH_2Cl_2 solution. Under glassy conditions a number of unresolved signals are detected, five of which display important spectral intensities. On the basis of the rhombic patterns of the preceding Rh(II) complexes (in particular, their anisotropic ΔH_i values), three of the five most intense signals can be reasonably attributed to $[(\eta^5\text{-}C_9H_2Me_5)Rh(1,5\text{-}C_8H_{12})]^+$ under the assumption of a "three g_{aniso}" spectral pattern, basically representative of low spin and unsymmetrical Rh(II) centres. The experimental g_i and related $\delta g_{\ell-h}$ values significantly differ from those of the above mentioned Rh(II) derivatives; moreover, the two high-field signals are noticeably overlapped and broadened. In addition, the rhombic lineshape exhibits anisotropic features (g_i and $\delta g_{\ell-h}$) suggestive of a reduced metallic nature. Further, the high-field absorption exhibits in the third derivative mode a poorly resolved multiplet of five signals which can be attributed to the shpf interaction of the $S = 1/2$ unpaired electron with the four magnetically equivalent ^1H nuclei of the $(1,5\text{-}C_8H_{12})$ ligand. In

Table 3
Temperature dependent X-band EPR parameters of the Rh(II) complexes under study [$\langle g \rangle = 1/3(g_\ell + g_m + g_h)$; $\langle a \rangle = 1/3(a_\ell + a_m + a_h)$; $\delta g_{\ell-h} = g_\ell - g_h$; g_i: ±0.008; a_i: ±2G]

Complex (solvent)	g_ℓ	g_m	g_h	$\langle g \rangle$	g_{iso}	a_ℓ	a_m	a_h	$\langle a \rangle$	a_{iso}	$\delta g_{\ell-h}$
$[(C_9H_2Me_5)Rh(C_6Me_6)]^+$ (PC)	2.095	1.995	1.850	1.980	1.979	15.0	7.0	$\leqslant$30.0[a]	$\leqslant$17.3[a]	$\leqslant$20.0[a]	0.245
$[(C_9H_2Me_5)Rh(C_5H_5)]^0$ (PC)	2.078	1.994	1.830	1.967		$\leqslant$17.0[a]	8.0	$\leqslant$33.0[a]	$\leqslant$19.3[a]		0.248
$[(C_9H_7)Rh(C_5Me_5)]^0$[b] (THF)	2.012	1.846	1.846	1.901	1.96						
$[(C_9H_2Me_5)Rh(C_8H_{12})]^+$ (CH_2Cl_2)	2.076	2.002	1.990	2.023	2.047	$\leqslant$12.0[a]	$\leqslant$12.0[a]	$\leqslant$10[a]	$\leqslant$11.3[a]	$\leqslant$28.0[a]	0.086

[a] ΔH_{exp}.
[b] From Ref. [23].

summary, the EPR features suggest that $[(\eta^5\text{-}C_9H_2Me_5)Rh(1,5\text{-}C_8H_{12})]^+$ possesses a minor metallic character than $[(C_9H_2Me_5)Rh(C_6Me_6)]^+$ and $[(C_9H_2Me_5)Rh(C_5H_5)]^0$.

At the glassy-fluid transition, the anisotropic features drop out and the solution exhibits in the first derivative mode a relatively broad and unresolved isotropic signal. The second and third derivative spectra evidentiate a noisy and poorly separated doublet in the limit of the experimental linewidth, which can be attributed to the direct interaction of the unpaired spin density with the rhodium nucleus. Accordingly, the g_{iso} value fits the related glassy $\langle g \rangle$ one. As a confirmation, rapidly refreezing the fluid solution partially recovers the previous rhombic pattern.

2.5. Rhodium–benzene bonding in $[(ring)Rh(C_6H_6)]^{2+}$ complexes

In order to understand dependence of the rhodium–benzene bonding upon ring ligand in $[(ring)Rh(C_6H_6)]^{2+}$ (ring = Cp, Cp*, C_9H_7, $C_9H_2Me_5$), we have carried out their fragment analysis using energy decomposition scheme [30], one of the best methods for analyzing the chemical bond. In particular, using this method Frenking et al. have clarified the bonding situation in sandwich compounds of iron and chromium [31]. As can be seen from Table 4, the Rh–C_6H_6 interaction energies ΔE_{int} for cyclopentadienyl (Cp, Cp*) complexes are higher than those for indenyl (C_9H_7, $C_9H_2Me_5$) analogues, the energies being lower for methylated derivatives. The ΔE_{int} values correlate well with the Rh $\cdots$ C_6H_6 distances. The dissociation energies D_e are changed in the same order since the preparation energy ΔE_{prep} is nearly the same for all complexes. Noteworthy, $[(ring)Rh]^{2+}$ fragments with stronger Rh-ring interaction form poorer Rh–C_6H_6 bonds. Loosening of the latter for methylated derivatives mainly comes from decrease of orbital interactions. Finally, the energy partitioning suggests that the bonding interaction has predominantly covalent character (57–64%).

We also carried out the charge decomposition analysis [32] (Table 5). Donation from the benzene ligand to the $[(ring)Rh]^{2+}$ fragment for cyclopentadienyl complexes is higher than that for indenyl analogues, the donation being decreased upon methylation. Back donation is very close for both types of complexes, being smaller for the methylated derivatives. Comparing pairs of Cp/Cp* and C_9H_7/$C_9H_2Me_5$ complexes, one can notice that the decrease of donation from benzene (6-electron ligand) is connected with increase of donor properties of 5-electron ligand, in accordance with trans-effect. Further comparison of Cp/C_9H_7 and Cp*/$C_9H_2Me_5$ complexes allows to conclude that the indenyl ligands in the Rh(III) complexes studied are better donors than the cyclopentadienyls, similar to Rh(I) derivatives [9,10,33].

In order to get straightforward information about donor ability of $[ring]^-$ anions, we also carried out charge decomposition of the arene complexes into $[ring]^-$ and $[(C_6H_6)Rh]^{3+}$ fragments. The donation values do not confirm the conclusion made, however one should take into

Table 4
Energy decomposition analysis of $[(ring)Rh(C_6H_6)]^{2+}$ using fragments $[(ring)Rh]^{2+}$ and C_6H_6 at the BP86/TZ2P level (E in kcal mol^{-1})

	Cp	Cp*	C_9H_7	$C_9H_2Me_5$
ΔE_{int}	−123.75	−88.04	−101.38	−80.79
ΔE_{Pauli}	142.73	142.92	148.70	147.78
ΔE^{a}_{elstat}	−96.21 (36%)	−95.39 (41%)	−99.01 (40%)	−98.17 (43%)
ΔE_{orb} [a]	−170.28 (64%)	−135.56 (59%)	−151.07 (60%)	−130.40 (57%)
ΔE_{prep}	5.20	4.87	4.83	4.92
D_e	118.55	83.17	96.55	75.87
ΔE_{int}(Rh-ring) in $[(ring)Rh]^{2+}$	−1011.60	−1095.49	−1028.97	−1081.85
Rh $\cdots$ C_6H_6 (Å)[b]	1.822	1.857	1.836	1.861
	1.788	*1.819*	*1.799*	*1.821*
		(1.766[c])		(1.776[d])

[a] The values in parentheses give the percentage contribution to the total attractive interactions.
[b] Values at the PBE/bazis4 level are given in *italics*.
[c] XRD for $[Cp^*Rh(C_6H_5Me)]^{2+}$ [17].
[d] XRD for **3c**.

Table 5
Charge decomposition analysis of $[(ring)Rh(C_6H_6)]^{2+}$ complexes and rhodium NBO charges at the BP86/TZVPP-def2//BP86/TZ2P level (all values in a.u.)

	Cp	Cp*	C_9H_7	$C_9H_2Me_5$
Donation $C_6H_6 \rightarrow [(ring)Rh]^{2+}$	1.156	1.090	1.106	1.054
Back donation $[(ring)Rh]^{2+} \rightarrow C_6H_6$	0.358	0.340	0.366	0.334
Net charge donation $C_6H_6 \rightarrow [(ring)Rh]^{2+}$	1.169	0.934	1.049	0.879
Donation $[ring]^- \rightarrow [(C_6H_6)Rh]^{3+}$	1.194	1.028	1.048	0.998
Back donation $[(C_6H_6)Rh]^{3+} \rightarrow [ring]^-$	0.296	0.242	0.262	0.212
Net charge donation $[ring]^- \rightarrow [(C_6H_6)Rh]^{3+}$	2.045	2.303	2.145	2.356
q_{Rh}	0.487	0.463	0.495	0.474

Table 6
Calculated reaction energies (kcal mol^{-1}) at the PBE/bazis4 level (ZPE corrected values are given in parentheses)

Reaction	Cp	Cp*	C_9H_7	$C_9H_2Me_5$
$[(ring)Rh(C_6H_6)]^{2+} + 3MeCN \rightarrow [(ring)Rh(MeCN)_3]^{2+} + C_6H_6$	−68.890	−58.823	−64.696	− 58.941
	(−66.793)	(−56.497)	(−62.618)	(−56.133)
$[(ring)Rh(C_6H_6)]^{2+} + MeCN \rightarrow [(ring)Rh(C_6H_6)](MeCN)]^{2+}$	−14.748	−12.492	−15.505	−16.234
	(−14.551)	(−12.076)	(−15.043)	(−15.548)
$[(ring)Rh(C_6H_6)]^{2+} + 3MeCN \rightarrow [Rh(MeCN)_6]^{3+} + [ring]^-$	230.616	262.430	218.634	242.277
	(231.168)	(262.043)	(219.769)	(242.808)

account that these values include both charge donation and electronic polarization contributions. Indeed, net charge donation between the fragments (defined as a difference between charge transfers in two directions without polarization terms [34]) shows that donor ability is increased in the following order: $Cp > C_9H_7 > Cp^* > C_9H_2Me_5$. At the same time, the NBO charge at the Rh atom (last entry in Table 5), is lower for cyclopentadienyl complexes than for indenyl analogues, which can be explained by increase of net donation from the C_6H_6 ring. The lower rhodium charge for $[(\eta^5\text{-}C_5Me_5)Rh(C_6H_6)]^{2+}$ compared with **3a** is in accordance with easier reduction of the latter (vide supra).

Finally, we estimated energies of benzene replacement by acetonitrile (Table 6). The formation of tris(acetonitrile) complexes $[(ring)Rh(MeCN)_3]^{2+}$ is exothermic in all cases; the reaction energies for the cyclopentadienyl and indenyl complexes are close, being smaller for the methylated derivatives. It was supposed that the interaction of the benzene complexes with one MeCN molecule is the rate-determining step. This step is also exothermic, the process being more favorable for the indenyl derivatives as a consequence of indenyl effect [35]. These data explain easy solvolysis of cations $[(C_5R_5)Rh(C_6H_6)]^{2+}$ but do not explain unreactiveness of **3a** (vide supra), which possibly has kinetic origin caused by bulky $C_9H_2Me_5$ ligand. Further displacement of $[ring]^-$ proved to be endothermic suggesting stability of the $[(ring)Rh(MeCN)_3]^{2+}$ cations in acetonitrile.

3. Conclusion

The iodide complex **2** can be used as a convenient synthon of the fragment $(\eta^5\text{-}C_9H_2Me_5)Rh$ either directly or via intermediate transformation into labile nitromethane solvate. The arene–indenyl complexes **3a–c** proved to be much less reactive towards arene replacement by solvent molecules compared with cyclopentadienyl analogues. Complexes **3a–c** undergo reduction at more positive potential than Cp* derivatives in accordance with higher NBO charges at the rhodium atom.

4. Experimental

4.1. General

The reactions were carried out under an inert atmosphere in dry solvents, unless otherwise stated. The isolation of products was conducted in air. Starting materials $[(1,5\text{-}C_8H_{12})RhCl]_2$ [36], $AgBF_4 \cdot 3$dioxane [37], and $CpRh(\eta^5\text{-}C_4H_4BPh)$ [38] were prepared as described in the literature. 1,2,3,4,7-Pentamethylindene was synthesized similar to 1,2,3-trimethylindene [39]. ^{1}H NMR spectra (δ in ppm) were recorded on a Bruker AMX-400 spectrometer (400.13 MHz) relative to residual protons of the solvents.

4.2. Synthesis of 1,2,3,4,7-pentamethylindene

p-Xylene (95 ml) and $AlCl_3$ (17.6 g, 131.8 mmol) were placed into a three neck 250 ml round bottom flask fitted with a magnetic stirring apparatus, an addition funnel, and a reflux condenser. The stirred mixture was cooled to 0 °C and tigloyl chloride (7.8 g, 65.8 mmol) was added dropwise during 15 min. After the addition was complete, the mixture was allowed to come to room temperature and then refluxed for 9 h. The mixture was cooled to room temperature and poured into a 1000 ml beaker containing 200 g of ice and 50 ml of concentrated hydrochloric acid. After 1 h the organic layer was removed and dried over anhydrous sodium sulfate. The excess *p*-xylene was removed in vacuo. The residue was eluated through a short silica gel column (10 cm) by petroleum ether. Yield 10.5 g (85%) of 2,3,4,7-tetramethyl-1-indanone as a yellow oil. ^{1}H NMR ($CDCl_3$): $\delta = 7.24$ (m, 1H, arom.), 7.03 (m, 1H, arom.), 3.48 (m, 1H, CH), 2.77 (m, 1H, CH), 2.61 (s, 3H, Me), 2.38 (s, 3H, Me), 1.36 (d, 1H, Me), 1.28 (d, 1H, Me), 1.25 (d, 2H, Me), 1.10 (d, 2H, Me).

A solution of 2,3,4,7-tetramethyl-1-indanone (10.5 g, 55.9 mmol) in ether (120 ml) was added to a 500 ml round bottom flask fitted with a magnetic stirring apparatus, an addition funnel, and a reflux condenser. Methyl lithium (75 ml, 0.98 M in diethyl ether, 73.5 mmol) was added dropwise during 30 min and the mixture was refluxed for 9 h. After cooling to 0 °C, 50 ml of saturated ammonium chloride solution was added dropwise. The organic layer was dried over sodium sulfate. The solvent was removed in vacuo to leave 9.6 g (84%) of 2,3,4,7-tetramethyl-1-indanol.

The mixture of 2,3,4,7-tetramethyl-1-indanol (1.68 g, 8.2 mmol) and I_2 (10 mg, 0.04 mmol) was stirred at 100 °C for 1 h. The reaction mixture was diluted by ether (50 ml) and washed by water solution of $Na_2S_2O_3$ (10%). The organic layer was dried over sodium sulfate and ether was removed in vacuo. The residue was chromatographed on silica column (1×20 cm). A light yellow band eluted

with petroleum ether was collected to give yellow oil after removal of solvent in vacuo. Yield 1.45 g (95%) of 1,2,3,4,7-pentamethylindene. The product is sufficiently pure and can be used for subsequent syntheses without purification. ^{1}H NMR ($CDCl_3$): $\delta = 6.93$ (d, 1H, arom.), 6.83 (d, 1H, arom.), 3.19 (q, 1H, CH), 2.58 (s, 3H, Me), 2.40 (s, 3H, Me), 2.23 (s, 3H, Me), 1.98 (s, 3H, Me), 1.27 (d, 3H, Me).

4.3. Synthesis of (η^5-$C_9H_2Me_5$)Rh(1,5-C_8H_{12}) (**1**)

A solution of BuLi in hexane (2.3 ml of 2.1 M solution, 4.83 mmol) was added to 1,2,3,4,7-pentamethylindene (884 mg, 4.75 mmol) in THF (25 ml). The reaction mixture was stirred for 24 h. [(1,5-C_8H_{12})RhCl]$_2$ (585 mg, 1.19 mmol) was added to solution obtained and the mixture was stirred additionally 2 h. The solvent was removed in vacuo. The residue was extracted by petroleum ether and filtered through layer of Al_2O_3 (3–5 cm). After evaporation in vacuo, the crude product was recrystallized from hot THF/MeOH (1:2). Yield 515 mg (55%) of **1** as yellow crystalline solid. Anal. Calc. for $C_{22}H_{29}Rh$: C, 66.66; H, 7.37. Found: C, 66.84; H, 7.41%. ^{1}H NMR ($CDCl_3$): $\delta = 6.56$ (s, 2H, $C_9H_2Me_5$), 3.44 (m, 4H, C_8H_{12}), 2.46 (s, 6H, $C_9H_2Me_5$), 2.19 (s, 3H, $C_9H_2Me_5$), 2.04 (s, 6H, $C_9H_2Me_5$), 1.87 (m, 4H, C_8H_{12}), 1.75 (m, 4H, C_8H_{12}).

4.4. Synthesis of [(η^5-$C_9H_2Me_5$)RhI_2]$_2$ (**2**)

A solution of I_2 (32 mg, 0.13 mmol) in ether (3 ml) was added to (η^5-$C_9H_2Me_5$)Rh(1,5-C_8H_{12}) (50 mg, 0.13 mmol) in the same solvent (5 ml) and reaction mixture was stirred for ca. 0.5 h (an inert atmosphere is not necessary). The black precipitate formed was centrifuged off and washed by ether. Yield: 69 mg (98%). Anal. Calc. for $C_{14}H_{17}I_2Rh$: C, 31.02; H, 3.16. Found: C, 31.23; H, 3.13%. ^{1}H NMR (DMSO-d_6): $\delta = 7.28$ (s, 2H, $C_9H_2Me_5$), 2.65 (s, 6 H, $C_9H_2Me_5$), 2.27 (s, 6H, $C_9H_2Me_5$), 2.13 (s, 3H, $C_9H_2Me_5$).

4.5. Synthesis of [(η^5-$C_9H_2Me_5$)Rh(arene)](BF_4)$_2$ (**3a**–**c**(BF_4)$_2$)

$MeNO_2$ (2 ml) was added to a mixture of **2** (80 mg, 0.07 mmol) and $AgBF_4 \cdot 3$dioxane (135 mg, 0.29 mmol). The reaction mixture was stirred for ca. 0.5 h. The precipitate of AgI that formed was removed by centrifugation and an excess of the arene (0.5 ml of C_6H_6 or C_6H_5OMe, or 100 mg of C_6Me_6) was added to the solution. The reaction mixture was stirred for ca. 24 h and the solvent was removed in vacuo. The residue was washed with CH_2Cl_2 (3×2 ml) and twice reprecipitated from nitromethane by ether. Compounds **3a**–**c** (BF_4)$_2$ were obtained as an orange solids.

3a(BF_4)$_2$, arene = C_6H_6. Yield: 75%. Anal. Calc. for $C_{20}H_{23}B_2F_8Rh$: C, 44.49; H, 4.29. Found: C, 44.15; H, 4.01%. ^{1}H NMR (nitromethane-d_3): $\delta = 7.71$ (s, 2H, $C_9H_2Me_5$), 7.28 (s, 6H, C_6H_6), 2.83 (s, 6H, $C_9H_2Me_5$), 2.77 (s, 6H, $C_9H_2Me_5$), 2.36 (s, 3H, $C_9H_2Me_5$).

3b(BF_4)$_2$, arene = C_6Me_6. Yield: 79%. Anal. Calc. for $C_{26}H_{35}B_2F_8Rh$: C, 50.04; H, 5.65. Found: C, 50.07; H, 5.64%. ^{1}H NMR (nitromethane-d_3): $\delta = 7.78$ (s, 2H, $C_9H_2Me_5$), 2.58 (s, 6H, $C_9H_2Me_5$), 2.47 (s, 6H, $C_9H_2Me_5$), 2.25 (s, 18H, C_6Me_6), 2.06 (s, 3H, $C_9H_2Me_5$).

3c(BF_4)$_2$, arene = C_6H_5OMe. Yield: 88%. Anal. Calc. for $C_{21}H_{25}B_2F_8ORh$: C, 44.28; H, 4.42. Found: C, 43.74; H, 4.19%. ^{1}H NMR (nitromethane-d_3): $\delta = 7.73$ (s, 2H, $C_9H_2Me_5$), 7.33 (m, 2H, C_6H_5OMe), 7.01 (d, 2H, C_6H_5-OMe), 6.94 (t, 1H, C_6H_5OMe), 3.92 (s, 3H, C_6H_5OMe), 2.78 (s, 12H, $C_9H_2Me_5$), 2.32 (s, 3H, $C_9H_2Me_5$).

4.6. Synthesis of [CpRh(μ-η^5:η^6-C_4H_4BPh)Rh(η^5-$C_9H_2Me_5$)](BF_4)$_2$ (**4**(BF_4)$_2$)

A mixture of **2** (60 mg, 0.06 mmol) and $AgBF_4 \cdot 3$dioxane (105 mg, 0.23 mmol) in $MeNO_2$ (1 mL) was stirred for 0.5 h at room temperature. The precipitate of AgI was centrifuged off and the solution obtained was added to CpRh(η^5-C_4H_4BPh) (35 mg, 0.11 mmol). The solution was stirred for 2 h. Ether (ca. 10 ml) was added. Red precipitate of **4**(BF_4)$_2$ was filtered off and washed by CH_2Cl_2. Yield 68 mg (78%). Anal. Calc. for $C_{29}H_{31}B_3F_8Rh_2$: C, 45.25; H, 4.06%. Found: C, 44.41; H, 3.92%. ^{1}H NMR (nitromethane-d_3): $\delta = 7.47$ (s, 2 H, $C_9H_2Me_5$), 7.15 (m, 3H, Ph), 7.09 (m, 2H, Ph), 5.61 (m, 2H, β-C_4H_4B), 5.34 (s, 5H, Cp), 4.54 (m, 2H, α-C_4H_4B), 2.66 (s, 6H, $C_9H_2Me_5$), 2.57 (s, 6H, $C_9H_2Me_5$), 2.25 (s, 3H, $C_9H_2Me_5$).

4.7. Synthesis of [(η^5-$C_9H_2Me_5$)RhCp]PF_6 (**5**PF_6)

Acetonitrile (3 ml) was added to a mixture of complex **2** (60 mg, 0.06 mmol) and CpTl (41 mg, 0.15 mmol). The reaction mixture was stirred for ca. 24 h and filtered. The solvent was removed in vacuo, and an excess of an aqueous solution of NH_4PF_6 was added to the residue. Suspension obtained was stirred ca. 0.5 h at 50–70 °C. The precipitate was filtered off, washed with water, and dried in vacuo. Reprecipitation from acetonitrile with ether gave complex **5**PF_6 (48 mg, 87%) as a yellow solid. Anal. Calc. for $C_{19}H_{23}F_6PRh$: C, 45.80; H, 4.45. Found: C, 45.77; H, 4.44%. ^{1}H NMR (acetone-d_6): $\delta = 7.08$ (s, 2H, $C_9H_2Me_5$), 5.69 (s, 5H, Cp), 2.71 (s, 6H, $C_9H_2Me_5$), 2.68 (s, 6H, $C_9H_2Me_5$), 2.28 (s, 3H, $C_9H_2Me_5$).

4.8. X-ray crystallography of [**3c**](BF_4)$_2$

Crystals of [**3c**](BF_4)$_2$ were grown up by slow diffusion in two-layer system, ether and a solution of complex in $MeNO_2$.

Crystal data: $C_{21}H_{25}B_2F_8ORh$ ($M = 569.94$), monoclinic, space group $P2_1/c$, $a = 7.9088(7)$, $b = 18.3275(17)$, $c = 15.6285(14)$ Å, $\beta = 95.272(2)°$, $V = 2255.7(4)$ Å^3, $Z = 4$, $d_{calc} = 1.678$ g cm^{-3}, $\mu = 0.834$ mm^{-1}, $F(000) = 1144$, crystal size $0.25 \times 0.35 \times 0.50$ mm.

X-ray diffraction experiment was carried out with a Bruker Apex II CCD area detector, using graphite

monochromated Mo Kα radiation ($\lambda = 0.71073$ Å, $1.72 < \theta < 28.00°$) at 120 K. Absorption correction was applied semi-empirically using APEX2 program ($T_{max}/T_{min} = 0.814/0.710$) [40]. The structure was solved by direct method and refined by the full-matrix least-squares technique against F^2 in anisotropic approximation for non-hydrogen atoms. All hydrogen atoms were refined in isotropic approximation in riding model with the $U_{iso}(H)$ parameters equal to 1.2 $U_{eq}(C_i)$ or 1.5$U_{eq}(C_{ii})$, where $U(C_i)$ and $U(C_{ii})$ are respectively the equivalent thermal parameters of the methyne and methyl carbon atoms to which the corresponding H atoms are bonded. The refinement converged to $wR_2 = 0.0983$ and GOF = 1.000 for all independent reflections ($R_1 = 0.0389$ was calculated against F for 4722 observed reflections with $I > 2\sigma(I)$). All calculations were performed using the SHELXTL software [41].

4.9. Electrochemistry and spectroelectrochemistry

Electrochemical measurements were performed in deaerated CH_2Cl_2 (Aldrich, anhydrous, 99.9%) or propylene carbonate (Aldrich, anhydrous, 99.7%) solutions containing $[NBu_4][PF_6]$ (0.2 mol dm^{-3}) as supporting electrolyte (Fluka, electrochemical grade). Cyclic voltammetry was performed in a three-electrode cell having a platinum or a gold working electrode surrounded by a platinum-spiral counter electrode and the aqueous saturated calomel reference electrode (SCE) mounted with a Luggin capillary. Either a BAS 100A or a BAS 100W electrochemical analyzers were used as polarizing units. Controlled potential coulometry was performed in a H-shaped cell with anodic and cathodic compartments separated by a sintered-glass disk. The working macroelectrode was a platinum gauze; a mercury pool was used as the counter electrode. All the potential values are referred to the saturated calomel electrode (SCE). Under the present experimental conditions the one-electron oxidation of ferrocene occurs at $E^{\circ\prime} = +0.39$ V ($\Delta E_p = 68$ mV at 0.2 V s^{-1}) in CH_2Cl_2 and at $E^{\circ\prime} = +0.37$ V ($\Delta E_p = 67$ mV at 0.2 V s^{-1}) in propylene carbonate.

The UV–Vis spectroelectrochemical measurements were carried out using a Perkin–Elmer Lambda 900 UV–Vis spectrophotometer and an OTTLE (optically transparent thin-layer electrode) cell [42] equipped with a Pt-minigrid working electrode (32 wires/cm), Pt minigrid auxiliary electrode, Ag wire pseudoreference and CaF_2 windows. The electrode potential was controlled during electrolysis by an Amel potentiostat 2059 equipped with an Amel function generator 568.

X-band EPR spectra were obtained by using a BRUKER ER 200-SRDD spectrometer ($\nu = 9.457$ GHz). The operational microwave frequency (Bruker Microwave bridge ER 401 MR) was tested with an XL Microwave Frequency Counter 3120 and the external magnetic field H_0 was calibrated by using a dpph powder sample ($g_{dpph} = 2.0036$). The temperature was controlled with a Bruker ER 4111 VT device (accuracy of ±1 °C).

4.10. Computational details

The geometry optimization was performed for C_s-symmetrical benzene complexes (with 2 eclipsed carbon atoms) at the BP86/TZ2P level of theory using the ADF (2006.01) program package [43]. Scalar relativistic effects were considered using the zero-order regular approximation (ZORA). All-electron basis sets optimized for ZORA calculations were used. The bonding interactions were analyzed by means of Morokuma–Ziegler energy decomposition scheme [44].

Charge decomposition analysis was carried out using the AOMix software [45]. The input files were obtained from single-point calculations at BP86/TZ2P optimized geometries with the GAUSSIAN 98 program [46] using BP86 functional and a basis set of triple-ζ quality with two polarization functions TZVPP-def2 [47]. Natural charges were obtained using the NBO scheme [48] at the same level of theory.

For the determination of energies of ligand replacement by acetonitrile, geometry optimization and frequency calculations were made using Priroda 6 software [49] at the PBE/basis4 level with four-component scalar-relativistic approximation.

Acknowledgements

Financial support from the Division of General Chemistry and Material Sciences of RAS is gratefully acknowledged. P.Z. gratefully acknowledges the financial support of the University of Siena (PAR PROGETTI 2005).

Appendix A. Supplementary material

CCDC 649054 contains the supplementary crystallographic data for this paper. These data can be obtained free of charge from The Cambridge Crystallographic Data Centre via www.ccdc.cam.ac.uk/data_request/cif. Supplementary data associated with this article can be found, in the online version, at doi:10.1016/j.jorganchem.2007.10.006.

References

[1] C. White, P.M. Maitlis, J. Chem. Soc. A (1971) 3322.
[2] R.H. Houghton, M. Voyle, J. Chem. Soc., Chem. Commun. (1980) 884.
[3] S.L. Grundy, A.J. Smith, H. Adams, P.M. Maitlis, J. Chem. Soc., Dalton Trans. (1984) 1747.
[4] D.A. Loginov, M.M. Vinogradov, Z.A. Starikova, P.V. Petrovskii, A.R. Kudinov, Izv. Akad. Nauk, Ser. Khim. (2004) 1871, Russ. Chem. Bull. 53 (2004) 1949 (Engl. Transl.).
[5] L.S. Shul'pina, A.R. Kudinov, G. Süss-Fink, D.A. Loginov, G.B. Shul'pin, Neftekhimiya 45 (2005) 336 [Pet. Chem. 45 (2005) 309 (Engl. Transl.)].
[6] M. Corsini, S. Losi, E. Grigiotti, F. Rossi, P. Zanello, A.R. Kudinov, D.A. Loginov, M.M. Vinogradov, Z.A. Starikova, J. Solid State Electrochem. 11 (2007) 1643.
[7] A.K. Kakkar, N.J. Taylor, J.C. Calabrese, W.A. Nugent, D.C. Roe, E.A. Connaway, T.B. Marder, J. Chem. Soc., Chem. Commun. (1989) 990.
[8] A.K. Kakkar, S.F. Jones, N.J. Taylor, S. Collins, T.B. Marder, J. Chem. Soc., Chem. Commun. (1989) 1454.

[9] A.K. Kakkar, N.J. Taylor, T.B. Marder, J.K. Shen, N. Hallinan, F. Basolo, Inorg. Chim. Acta 198–200 (1992) 219.
[10] T.M. Frankcom, J.C. Green, A. Nagy, A.K. Kakkar, T.B. Marder, Organometallics 12 (1993) 3688.
[11] C. White, S.J. Thompson, P.M. Maitlis, J. Chem. Soc., Dalton Trans. (1977) 1654.
[12] D.A. Loginov, D.V. Muratov, P.V. Petrovskii, Z.A. Starikova, M. Corsini, F. Laschi, F.de B. Fabrizi, P. Zanello, A.R. Kudinov, Eur. J. Inorg. Chem. (2005) 1737.
[13] D.A. Loginov, D.V. Muratov, D.S. Perekalin, Z.A. Starikova, E.A. Petrovskaya, E.I. Gutsul, A.R. Kudinov, Inorg. Chim. Acta, in press. doi:10.1016/j.ica.2006.12.045.
[14] R.T. Baker, T.H. Tulip, Organometallics 5 (1986) 839.
[15] S.A. Westcott, A.K. Kakkar, G. Stringer, N.J. Taylor, T.B. Marder, J. Organomet. Chem. 394 (1990) 777.
[16] A.K. Kakkar, G. Stringer, N.J. Taylor, T.B. Marder, Can. J. Chem. 73 (1995) 981.
[17] M. Maekawa, N. Hashimoto, T. Kuroda-Sowa, Y. Suenaga, M. Munakata, Anal. Sci. 17 (2001) 1361.
[18] S. Ogo, H. Chen, M.M. Olmstead, R.H. Fish, Organometallics 15 (1996) 2009.
[19] M.J. Shaw, W.E. Geiger, J. Hyde, C. White, Organometallics 17 (1998) 5486.
[20] P. Zanello, Inorganic Electrochemistry. Theory, Practice and Application, RS · C, United Kingdom, 2003.
[21] S. Santi, L. Orian, C. Durante, A. Bisello, F. Benetollo, L. Crociani, P. Ganis, A. Ceccon, Chem. Eur. J. 13 (2007) 1955.
[22] C. Amatore, A. Ceccon, S. Santi, J.-N. Verpeaux, Chem. Eur. J. 3 (1997) 279.
[23] O.V. Gusev, L.I. Denisovich, M.G. Peterleitner, A.Z. Rubezhov, N.A. Ustynyuk, J. Organomet. Chem. 452 (1993) 219.
[24] W.J. Bowyer, J.W. Merkert, W.E. Geiger, A.L. Rheingold, Organometallics 8 (1989) 191.
[25] F.E. Mabbs, D. Collison, Electron paramagnetic resonance of d transition metal compoundsStudies in Inorganic Chemistry, vol. 16, Elsevier Ed., NY, 1992.
[26] T.M. Dunn, Trans. Faraday Soc. 57 (1961) 1441.
[27] G.P. Lozos, B.M. Hoffman, C.G. Franz, QCPE 11 (1974) 265.
[28] P. Piraino, G. Bruno, S. LoSchiavo, F. Laschi, P. Zanello, Inorg. Chem. 26 (1987) 2205.
[29] C. Bianchini, M. Peruzzini, F. Laschi, P. Zanello, Synthesis, Characterization and Chemistry of Rodium(II) Organometallic Complexes Stabilized by Tripodal Polyphosphine Ligands, vol. 14, Freund Publishing House Ltd., London, 1992.
[30] For recent reviews see (a) G. Frenking, N. Frohlich, Chem. Rev. 100 (2000) 717;
(b) G. Frenking, K. Wichmann, N. Frohlich, C. Loschen, M. Lein, J. Frunzke, V.M. Rayon, Coord. Chem. Rev. 238–239 (2003) 55;
(c) T. Ziegler, J. Autschbach, Chem. Rev. 105 (2005) 2695.
[31] (a) M. Lein, J. Frunzke, A. Timoshkin, G. Frenking, Chem. Eur. J. 7 (2001) 4155;
(b) J. Frunzke, M. Lein, G. Frenking, Organometallics 21 (2002) 3351;
(c) V. Rayón, G. Frenking, Organometallics 22 (2003) 3304.
[32] S. Dapprich, G. Frenking, J. Phys. Chem. 99 (1995) 9352.
[33] D. O'Hare, J.C. Green, T.B. Marder, S. Collins, G. Stringer, A.K. Kakkar, N. Kaltsoyannis, A. Kuhn, R. Lewis, C. Mehnert, P. Scott, S. Pugh, Organometallics 11 (1992) 48.
[34] S.I. Gorelsky, S. Ghosh, E.I. Solomon, J. Am. Chem. Soc. 128 (2006) 278.
[35] M.E. Rerek, L.-N. Ji, F. Basolo, J. Chem. Soc., Chem. Commun. (1983) 1208.
[36] G. Giordano, R.H. Crabtree, Inorg. Synth. 19 (1979) 218.
[37] M.E. Woodhouse, F.D. Lewis, T.J. Marks, J. Am. Chem. Soc. 104 (1982) 5586.
[38] G.E. Herberich, U. Büschges, B. Hessner, H. Lüthe, J. Organomet. Chem. 312 (1986) 13.
[39] T.E. Ready, J.C.W. Chien, M.D. Rausch, J. Organomet. Chem. 583 (1999) 11.
[40] Bruker (2005). APEX2 softwarwe package, Bruker AXS Inc., 5465, East Cheryl Parkway, Madison, WI 5317.
[41] G.M. Sheldrick, SHELXTL v. 5.10, Structure Determination Software Suite, Bruker AXS Inc., Madison, WI, USA, 1998.
[42] M. Krejčik, M. Daněk, F. Hartl, J. Electroanal. Chem. 317 (1991) 179.
[43] F.M. Bickelhaupt, E.J. Baerends, Rev. Comput. Chem. 15 (2000) 1.
[44] (a) K. Morokuma, Chem. Phys. 55 (1971) 1236;
(b) T. Ziegler, A. Rauk, Theor. Chim. Acta 46 (1977) 1;
(c) F.M. Bickelhaupt, E.J. Baerends, in: K.B. Lipkowitz, D.B. Boyd (Eds.), Rev. Comput. Chem, vol. 15, Wiley-VCH, New York, 2000, p. 1.
[45] S.I. Gorelsky, AOMIX program, http://www.sg-chem.net.
[46] M.J. Frisch, G.W. Trucks, H.B. Schlegel, G.E. Scuseria, M.A. Robb, J.R. Cheeseman, V.G. Zakrzewski, J.A. Montgomery Jr., R.E. Stratmann, J.C. Burant, S. Dapprich, J.M. Millam, A.D. Daniels, K.N. Kudin, M.C. Strain, O. Farkas, J. Tomasi, V. Barone, M. Cossi, R. Cammi, B. Mennucci, C. Pomelli, C. Adamo, S. Clifford, J. Ochterski, G.A. Petersson, P.Y. Ayala, Q. Cui, K. Morokuma, D.K. Malick, A.D. Rabuck, K. Raghavachari, J.B. Foresman, J. Cioslowski, J.V. Ortiz, A.G. Baboul, B.B. Stefanov, G. Liu, A. Liashenko, P. Piskorz, I. Komaromi, R. Gomperts, R.L. Martin, D.J. Fox, T. Keith, M.A. Al-Laham, C.Y. Peng, A. Nanayakkara, C. Gonzalez, M. Challacombe, P.M.W. Gill, B.G. Johnson, W. Chen, M.W. Wong, J.L. Andres, M. Head-Gordon, E.S. Replogle, J.A. Pople, Gaussian 98 (Revision A.6), Gaussian Inc., Pittsburgh, PA, 1998.
[47] (a) F. Weigend, R. Ahlrichs, Phys. Chem. Chem. Phys. 7 (2005) 3297;
(b) http://www.ipc.uni-karlsruhe.de/tch/tch1/TBL/tbl.html.
[48] A.E. Reed, L.A. Curtiss, F. Weinhold, Chem. Rev. 88 (1988) 899.
[49] (a) D.N. Laikov, Chem. Phys. Lett. 281 (1997) 151;
(b) D.N. Laikov, Chem. Phys. Lett. 416 (2005) 116;
(c) D.N. Laikov, Y.A. Ustynyuk, Russ. Chem. Bull. 54 (2005) 820;
(d) The Priroda 6 program can be obtained free of charge from its author Dr. Dmitry Laikov (E-mail address: laikov@physto.se).